Fabrication of high efficient organic/CdSe quantum dots hybrid OLEDs by spin-coating method

A. Uddin* and C. C. Teo[1]
School of Photovoltaic and Renewable Energy Engineering,
The University of New South Wales, Sydney 2052, Australia
[1]School of Materials Science and Engineering,
Nanyang Technological University; Singapore 639798

ABSTRACT

The cadmium selenite (CdSe) quantum dots (QDs) have promising applications in display technology since its luminescence wavelength can be tuned precisely from blue to red by changing the diameter of the core from 2.0 to 7.0 nm. A self-assembled monolayer of QDs, sandwiched between two organic thin films is necessary to isolate the luminescence processes from charge conduction. The use of QDs for device technology, one of the fundamental issues is how to distribute QDs uniformly on patterned surfaces with precise control of density. In this study, we demonstrate that uniform distribution of QDs with controllable density can be achieved using the conventional spin-coating method. We have fabricated high efficient QD-OLED by spin-coating method. The estimated QDs threshold concentration was found ~ $9x10^{11}$ cm^{-2} for the best performance of QD-OLED. The AFM morphological studies of the hybrid device showed the formation of a disordered QD film as a result of the aggregation of CdSe/ZnS QDs upon phase segregation. The analysis of electroluminescence (EL) and photoluminescence (PL) performance of OLED showed that precise control of the QD concentration is necessary to maximize the coverage of QDs on organic surface which is an important factor in color tuning. The peak energies of the EL and PL showed only small spectral shifts and no significant dependence on the QD-concentration. The QD emission was increased about three times by annealing of QD-OLED.

Keywords: Quantum dot, Light emitting diodes, Organic/inorganic hybrid, Self-assembly

1. INTRODUCTION

Recently semiconductor quantum dots (QDs) materials have attracted great attention for the scientific and technological interest mostly because of their size-dependent optical and electronic properties. Among them cadmium selenite (CdSe) QDs have promising applications in display technologies since its luminescence wavelength can be tuned precisely from blue to red by changing the diameter of the core from 2.0 to 7.0 nm.[1] Compare to organic emitters, inorganic semiconductor QDs have a number of advantages such as high photo-stability and narrow emission line width.[2] The CdSe QD has narrow emission spectra e.g. full width half maximum (FWHM) ~30 nm, compared to those of inorganic phosphors make them outstanding sources of nearly pure color emission.[3] The environmental stability of CdSe QDs suggests that the device lifetimes of hybrid inorganic/organic light emitting diodes (QD-LEDs) should be much longer than pure organic light emitting diodes (OLEDs). The CdSe based QD-OLEDs could satisfy the technological requirements of flat panel displays and imaging application which require the narrowband emission characteristics as well as the efficient emission of visible light. The QD-LEDs is a keen technology for flat panel display for highly saturated color emission.

The combination of CdSe QDs luminescence properties with the advantages of organic processing techniques can be possibility to fabricate large area visible light emitters with physical properties of nano-scale.[1,4,5] The charge conductivity of closely packed QDs film is poor, making inefficient electrical pumping of

Organic Photonic Materials and Devices XV, edited by Christopher E. Tabor, François Kajzar, Toshikuni Kaino, Yasuhiro Koike, Proc. of SPIE Vol. 8622, 86220X · © 2013 SPIE · CCC code: 0277-786X/13/$18
doi: 10.1117/12.2001963

QD.[6] A single self-assembled QDs monolayer, sandwiched between two organic thin films is necessary to isolate the luminescence processes from charge conduction. The QD will function as both lumophores and charge transport layers in the device. The use of QDs for device technology, one of the fundamental issues is how to distribute QDs uniformly on patterned surfaces with precise control of density. In this paper, we have demonstrated the uniform distribution of CdSe/ZnS QDs with controllable density by using the conventional spin-coating method. We used a self-assembled monolayer of QDs, sandwiched between two thin films of organic layers on indium-tin-oxide (ITO) coated glass substrate for the QD-OLED fabrication. The effects of process parameters on QDs concentration as well as tuning of QD-OLED performances were investigated. There was a QD threshold concentration below which there was no emission from the QDs in QD-OLED. The estimated QD concentration was found as ~ $9x10^{11}$ cm^{-2} for the best performance of QD-OLED. The emission intensity of QD-OLED was increased about three times by annealing at 80 °C for about 20 minutes at nitrogen atmosphere. The estimated highest external quantum efficiency (EQE) of QD-OLED was around 2.1%. The QD electroluminescence peak energy was remained same before and after the annealing of QD-OLED.

2. EXPERIMENTAL DETAILS

The investigated hybrid QD-OLED structure was composed of a monolayer of 5 nm size CdSe/ZnS quantum dots (QDs) (as purchased from Evident Technologies, NY, passivated with trioctylphosphine oxide (TOPO)) sandwiched between N,N'-diphenyl-N,N'-bis(3-methylphenyl)-(1,1'-biphenyl)-4,4'-diamine (TPD) and tris-(8-hydroxyquinoline) aluminium (Alq_3) on glass substrates coated with a semitransparent indium tin oxide (ITO) electrode as shown in Fig. 1(a). Two highly pure (99.9 %) chemicals TPD and Alq_3 were purchased from Aldrich-Sigma for this experiment. The QD, TPD and Alq_3 materials were confirmed by observing their absorption and emission spectra as shown in Fig. 1(b).

The QD solution was mixed with TPD dissolved in chloroform and spin-coated onto the ITO surface in a single step. Different QD concentrations from 0.25 mg/ml to 5.0 mg/ml were prepared and mixed with TPD dissolved in chloroform in different proportions. Nine hybrid samples were prepared with increasing CdSe/ZnS QDs concentration. The self-assembled QD layer was formed after the phase segregation of the QDs from TPD.[7,8] The phase segregation of QDs layer from TPD is shown in Fig. 2 by atomic force microscopy (AFM). The formation of monolayer thick self-assembled QDs on top of a ~ 30 nm thick TPD layer was determined by Rutherfurd Back Scattering (RBS) measurements. Subsequently around 50 nm thick Alq_3 layer was thermally evaporated on top of the QD layer before the Al cathode layer deposition. The Alq_3 depositions were performed at a high vacuum of 3×10^{-6} Torr and the deposition rate was fixed at about 1.5 Å/s.[9] The thickness of the Alq_3 film was monitored by a crystal monitor. Around 70 nm thick Al cathode layer was deposited in the last step of the device fabrication by using a JOEL JEE-400 Vacuum Evaporator. Similar OLED structure was also fabricated with organic layers without QDs for the comparison with hybrid devices as shown in Fig 1(a). We prepared 10 samples at a time on a substrate, each with an active area of 3x3 mm^2. All measurements were performed in air on non-encapsulated devices, but samples were stored and saved under nitrogen atmosphere. All measurements were done within two days after the device fabrication.

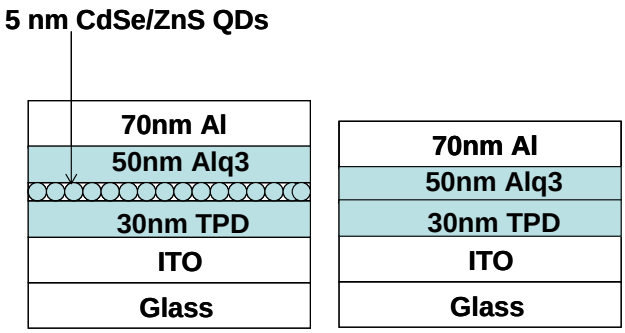

(a)

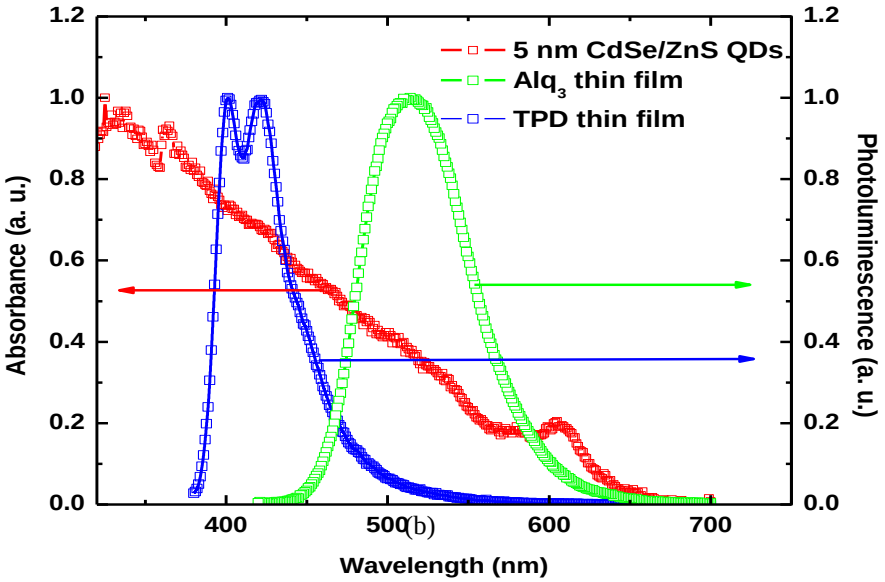

Figure 1: (a) The structure of QD-OLED on ITO coated glass substrate. A single layer of 5 nm size CdSe/ZnS QDs is sandwiched between 30 nm thick TPD and 50 nm thick Alq_3 layers. A similar structure of OLED was also grown without QD for comparison. (b) Absorption and emission spectra of 5 nm size CdSe/ZnS QDs, TPD and Alq_3 for confirmation of the materials.

The topography of self-assembled QD layer was characterized using AFM from Digital Instruments Nanoscope as shown in Fig. 2. We measured electroluminescence (EL), current-voltage (I-V) and light-current (L-I) characteristics of QD-OLEDs at room temperature by the Keithley source meter 2400 model and Minolta Luminance meter LS110. The QD-OLEDs were annealed at different temperatures for 20 minutes at nitrogen atmosphere to investigate the annealing effect.

3. EXPERIMENTAL RESULTS

AFM images in Fig. 2 shows the formation of segregated uniform dispersion of single QD layer on TPD apart from some aggregation. The QD density and the size of the aggregates can be varied by controlling the process parameters such as spin speed, density of QD solution, etc. The aggregates disappeared at the higher QD concentration typically when we used around 2.5 mg/ml CdSe/ZnS QDs solution. Generally, the QD density decreases with increasing spin speed and lower the coverage of TPD surface. The QD concentrations were estimated from the AFM images for different QD solution concentrations. The QD concentration was linearly increased with solution concentration up to 3.0 mg/ml as shown in Fig. 3. After that the QD concentration was become nearly constant due to the formation of multi-layers. We selected several concentrations of QD solutions such as 0.25, 0.50, 1.0, 1.50, 2.00, 2.5, 3.00, 4.00 and 5.00 mg/ml for the formation of self-assembly QD single layer at a spin speed of 5000 rpm for the fabrication of QD-OLEDs as shown in Fig. 1(a).

The aggregation can be attributed to spinodal phase separation that is triggered by the increase of interaction between QDs when a good solvent such as chloroform is replaced by air. In the absence of the solvent, the QDs experience a stronger Van der Waals attraction due to less dielectric shielding of solvent molecules. The QD density and the average size of the aggregates can be varied by controlling the process parameters. These observed patterns are due to the coalescence of the QD droplets before drying. It is suggested that the first nanocrystal layer is yellow and the second layer is white in the AFM images. The aggregates disappeared at the higher QD concentration typically around the 2.5 mg/ml CdSe/ZnS QDs solution. Different surface morphology was observed with different spin speed. Generally, the QD density decrease with increasing the spin speed and lower the coverage of surface.

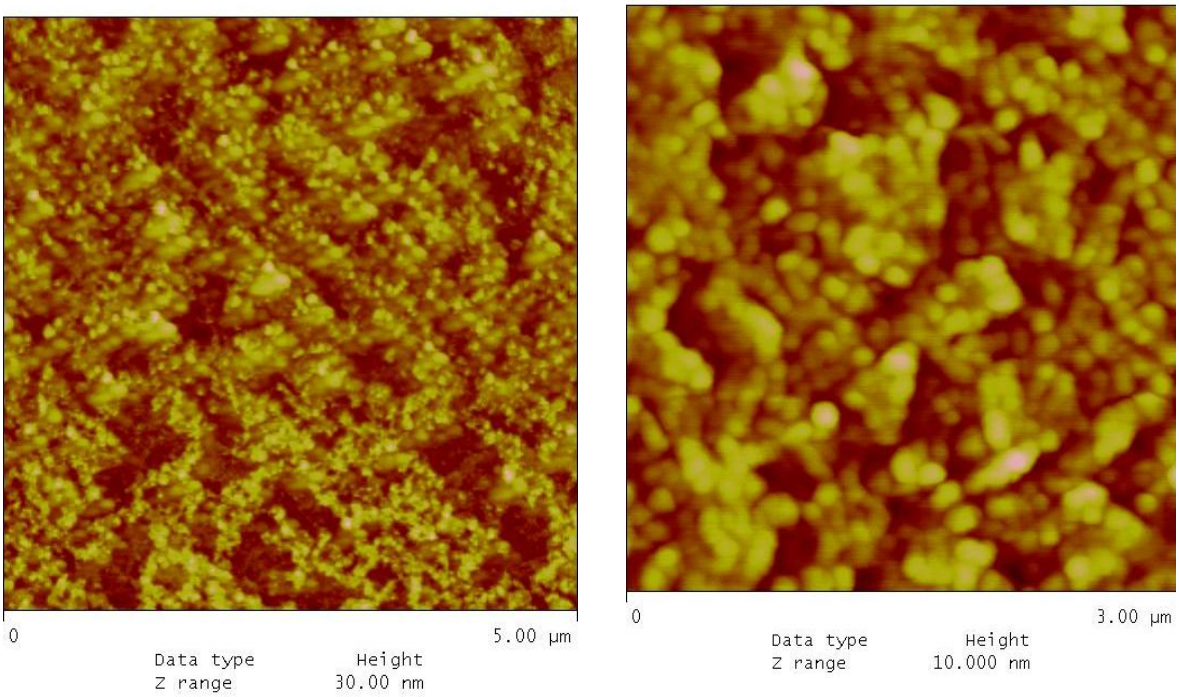

Figure 2: 5×5 µm (left) and 3x3 µm (right) AFM images of 5 nm size QDs on TPD/ITO layers on glass substrate for the 2.5 mg/ml solution of CdSe/ZnS QDs in chloroform as dropped and spin-coated at 5000 rpm

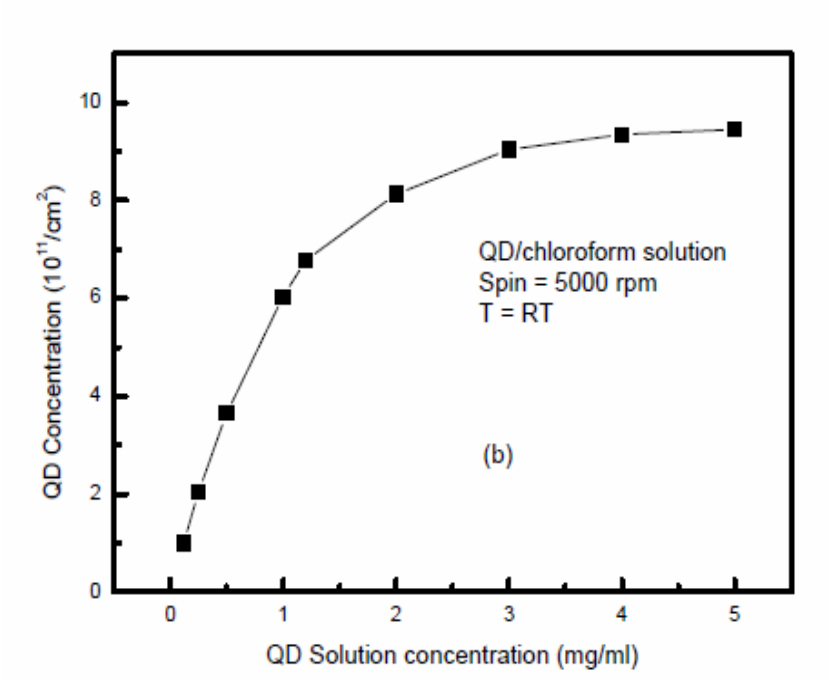

Figure 3: The plot of estimated QD concentration from AFM images on TPD layer as a function of QD solution concentration

The EL spectra of QD-OLEDs were measured at room temperature at 25 V bias for different concentrations of QDs on TPD layer as shown in Fig. 4. There is a QD threshold concentration below which there was no emission from the QDs. At low QD concentrations we have only observed green emission (~ 530 nm) from Alq_3 layer as the QD layer could not covered the all area of the device cross-section. However the red emission (~ 630 nm) from the QDs became visible at the higher QD concentrations (onset of QD emission from 1.5 mg/ml solution) with green emission due to the corresponding increase in area coverage. The 2.5 mg/ml QDs solution was produced the highest intensity QD-OLED. The organic EL was due to the presence of voids, grain boundaries, and interstitial spaces in the QD monolayers that allow the creation of excitons on organic sites.[8] With increasing QD coverage, there will be a larger absorption cross-section to maximize the energy from the organic molecules to QDs. Excitons generated at a distance more than the Förster energy transfer radius away from the QD in Alq_3 will also result in organic EL.[5,10] In addition, the higher holes injection rate into the Alq_3 layer at the higher electric field (e.g. 25 V bias) increased the organic emission. The QD emission stays dominant until breakdown occurred.

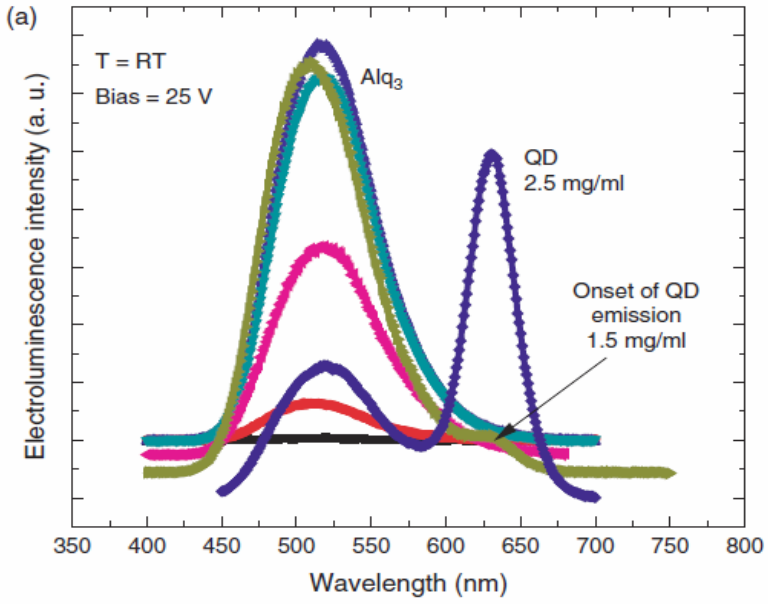

Figure 4: The EL spectra of QD-OLED for different QD concentrations at room temperature (RT) at 25 voltage bias. There is a QD threshold concentration below that we cannot observe the QD emission. The EL intensity of high concentration (2.5 mg/ml) QD-OLED was increased about three times after annealing.

When the high intensity QD-OLED was annealed at 80 °C for 20 minutes at nitrogen atmosphere we observed very strong red emission from the QD under the same bias voltage. The green emission from the Alq_3 layer was almost disappeared. The QD emission becomes nearly three times stronger after the annealing. This strong QD emission is an evident that the direct injection and recombination of carriers in QD. The mechanism of this improvement is not understood. The annealing temperature was just above the glass transition temperature (T_g) of TPD (~ 65 °C) but well below the T_g of Alq_3 (~ 170 °C).[12,13] The re-arrangement of QDs in the TPD/Alq_3 interface may take place during the annealing to form a more uniform layer which we realized in the suppression of Alq_3 emission. Annealing may also help to improve the QD surface morphology and the loss of some of the QD surface ligands.[11] The estimated QD concentration was found around $9x10^{11}$ cm^{-2} for the best performance of QD-OLED.

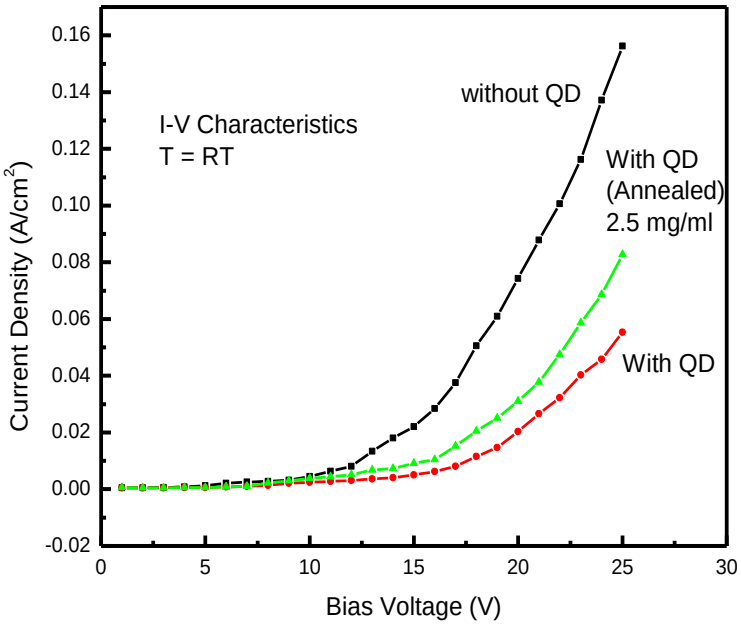

Figure 5: The I – V characteristics of high concentration (2.5 mg/ml) QD-OLED before and after the annealing. The I-V characteristic of OLED without QD at room temperature for comparison.

We measured the I-V characteristics of the best performance QD-OLED before and after the annealing as shown in Fig. 5. The I-V characteristics of an OLED without QD layer is also plotted with the QD-OLED for comparison. The current density was lower in QD-OLED compared to OLED for the same bias voltage due to the poor conductivity nature of QD layer. The current density of QD-OLED was increased after the annealing. We did not use any interface layer such as LiF between the electrode (Al) and the organic layer (Alq_3) to reduce the interface barrier between the electrode and organic layer.[14] In the electroluminescence characteristics of QD-OLED, the emission intensity nearly exponentially increases with current density up to ~ 1 x 10^{-2} (A/cm^2) as shown in Fig. 6. The emission intensity is almost saturated after the current density of ~1.5x10^{-2} (A/cm^2). The highest EQE of QD-OLED was around 2.1% after annealing. The observed luminance intensity of QD-OLED is comparable with the reported high performance QD-OLED.[4,8]

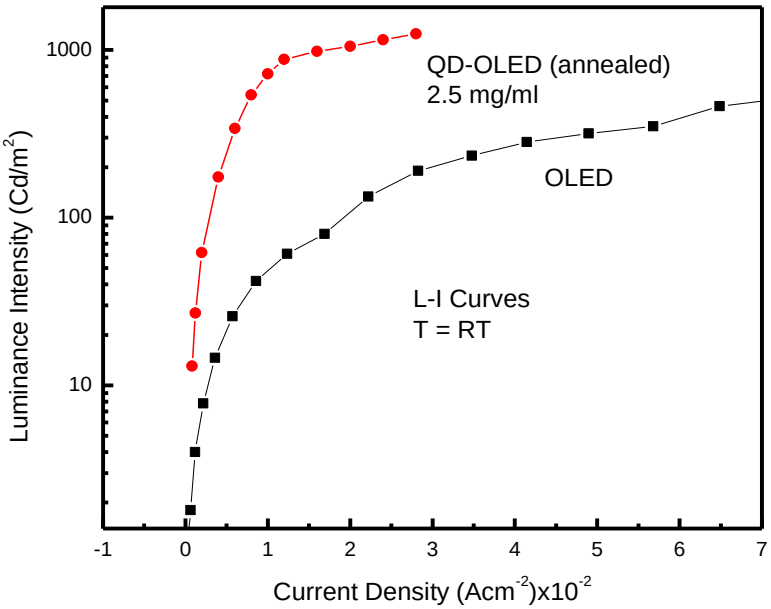

Figure 6: The plot of QD-OLED luminance intensity after annealing as a function of current density at room temperature. The luminescence intensity was around 1000 Cdm^{-2} at around 1x10^{-2} A/cm^2 current density. The L-I curve of an OLED without QD at room temperature is also plotted for comparison.

4. DISCUSSIONS

The work function of different layers in QD-OLED as shown in Fig. 7 is known from the previous studies.[15,16] The holes are considered to be injected from the ITO electrode to QDs through the TPD layer. Similarly, the electrons are injected from the Al cathode to QDs through the Alq_3 layer. The carrier injection from the electrodes depends on the bias voltage due to the interface barriers of different layers. The interface barrier can be defined by the difference in energy levels (valence and conduction bands offsets) between the electrode and the QD. When the applied bias voltage exceeds the interface barrier height (band-edge offsets) the injection of electrons and holes occurs into the QD. The electrons and holes transport by hopping mechanism from one sit to another through Alq_3 and TPD layers, respectively, to accumulate at the QD interfaces. This induces a charge gradient buildup on both sides of the QDs interface and generates a strong electric field across the QD junction. The presence of the higher band gap ZnS material coating on CdSe QD create an additional energy barrier at the interface between the organic and QD. The ZnS energy barrier becomes more effective in reducing injection of carriers into the QD core with thicker over-coating. The additional energy barrier of ZnS would counter balance the improvement of QDs carrier radiative recombination emission due to the better surface passivation of QDs by ZnS as well as for forming quantum wall trap centre for electrons and holes. This phenomenon shows that the EL process can be influenced by additional parameters besides surface passivation of the emitting cores. The annealing of QD-OLED device may reduce the interface barrier between the QDs and organics which we observed in the QD-OLED I-V characteristics in Fig. 5. The reduction of interface barriers increase electrons and holes injections into QD which we observed in the electroluminescence measurements of QD-OLED after annealing as shown in Fig. 4.

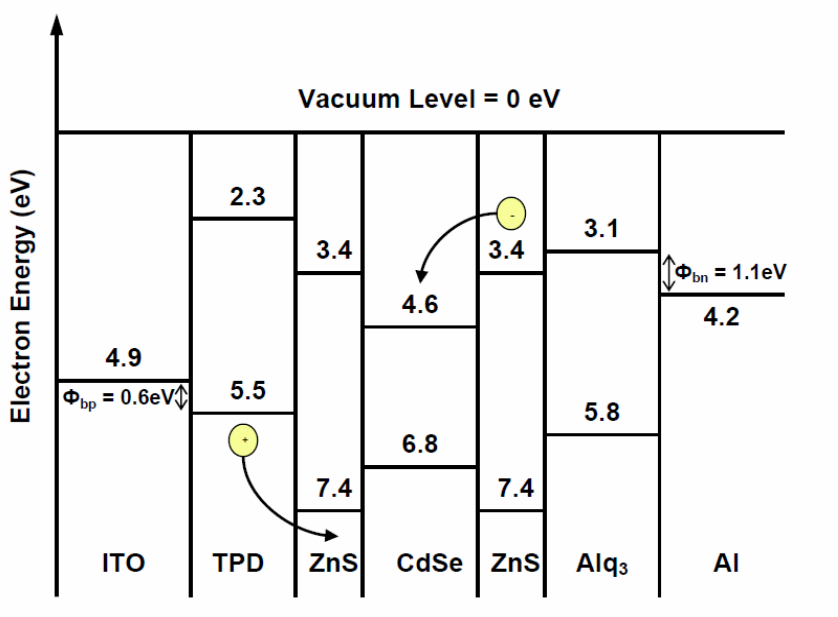

Figure 7: The schematic energy band diagram of QD-OLED showing the direct charge injection mechanism in device

The band diagram drawn in Figure 7 shows the energy difference between the conduction bands of the TPD and CdSe QDs is higher than that between the corresponding valence bands, i.e., E_c(TPD) – E_c(CdSe) = 2.3 eV compared to E_v(TPD) – E_v(CdSe) = 1.3 eV. That difference favours injection of holes from the TPD into the QDs over electrons into the TPD structure. The force migration of a small fraction of holes into the Alq_3 resulting in a contribution to the EL signal in the green region of the spectrum. The energy band diagram in Figure 5 shows that the presence of ZnS over coating is associated with an additional energy mismatch (energy barrier) at the interface between the organic and QD because of the higher band gap of ZnS.

5. Conclusions

The effects of CdSe/ZnS QD concentrations on the performance of self-assembly QD-OLEDs were investigated. Simple spin-coating method was used to fabricate the high performance QD-OLEDs. The uniform density of QDs on TPD layer was controlled by varying the QD solution concentrations with 5000 rpm speed of the spin coater. The estimated QD concentration was found ~ $9x10^{11}$ cm^{-2} for the best performance of QD-OLED. The annealing of QD-OLED was increased the QD emission intensity about three times than before annealing. The electroluminescence peak energy of QD was remained same before and after the annealing of QD-OLED. The effect of process parameters and the mechanism of QDs emissions are discussed.

ACKNOWLEDGEMENT

The authors would like to thanks the polymer lab technician at MSE/NTU for their supports. One of the authors (C.C. Teo) would like to thank NTU for his financial support. We are also grateful to all of our members for useful discussions and support in this work.

REFERENCES

1. S. Kim, B. Fisher, H. J. Eisler and M. Bawendi, "Type – II, Quantum dots: CdTe/CdSe (core/shall) and CdSe/ZnTe (core/shall) heterostructures", *J. Am. Chem. Soc. 125, 11466 (2003).*
2. Rogach, A.L., Semiconductor nanocrystal quantum dots: synthesis, assembly, spectroscopy and applications; Springer: wien, New York, 2008.
3. J. Zhao, J. Zhang, C. Jiang, J. Bohnenberger, T. Basche, and A. Mews, "Electroluminescence from isolated CdSe/ZnS quantum dots in multilayered light-emitting diodes", *J. Appl. Phys. 96, 3206 (2004).*
4. J. Kwak, W.K. Bae, M. Zorn, H. Woo, H. Yoon, J. Lim, S.W. Kang, S. Weber, H. J. Butt, R. Zentel, S. Lee, K. Char and C. Lee, "Characterization of quantum dot/conducting polymer hybrid films and their application in light emitting diodes", *Adv. Mater. 21, 5022 (2009).*
5. C.Y. Huang, Y. K. Su, T.C. Wen, T. F. Guo and M. L. Tu, "Single layered hybrid DBPPV-CdSe/ZnS quantum dot light-emitting diodes", IEEE Photon. Technol. Lett. 20, 282 (2008).
6. C. A. Leatherdale, C. R. Kagan, N.Y. Morgan, S.A. Empedocles, M.A. Kastner, M.G. Bawendi, *Phys. Rev. B62, 2669(2000*).
7. V. Bulovic, S. Coe, W. K. Woo, J. S. Steckel and M. Bawendi, "Tuning the performance of hybrid organic/inorganic quantum dot light emitting-diodes", *Organic Electronics 4, 123 (2003).*
8. S. C. Sullivan, W. K. Woo, J. S. Steckel, M. Bawendi and V. Bulovic, "Electroluminescence from single monolayers of nanocrystals in molecular organic devices", *Nature 420, 800 (2002)*.
9. C. B. Lee, A. Uddin, X. Hu and T. G. Andersson, "study of Alq3 thermal evaporation rate effects on the OLED", Mat. Sci. & Eng. B122, 14(2004).
10. K. Read, H. S. Karlsson, M. M. Murnane, H. C. Kapteyn and R. Haight, "Exciton dynamics of dye doped tris (8-hydroxy quinoline) aluminum films studied using time-resolved photoelectron spectroscopy", *J. Appl. Phys. 90 , 294(2001).*
11. Y.H. Niu, A.M. Munro, Y. J. Cheng, Y. Tian, M.S. Liu, J. Zhao, J. A. Bardecker, J. J. L. Plante, D.S. Ginger and A.K.Y. Jen, "Improve performance from multilayer quantum dot light emitting diodes via thermal annealing of the quantum dot layer", Adv. Mater. 19, 3371 (2007).
12. G. M. Credo, D. L. Winn and S. K. Buratto, "Near-field scanning optical microscopy of temperature and thickness dependent morphology and fluorescence in Alq3 films", *Chem. Mater. 13, 1258(2001).*
13. F. Khan, A. M. Hor and P. R. Sundararajan, "Influence of polycarbonate flexibility on the annealing induced phase separation of the hole transport molecule TPD in a model charge transport composition", *J. Phys. Chem. B 108, 117(2004).*
14. A. Uddin, C. B. Lee, X. Hu, and T. K. S. Wong, "Interface injection-limited carrier-transport properties of Alq3", *Appl. Phys. A78, 401 (2004).*
15. H. Mattoussi, L. H. Radzilowski, B. O. Dabbousi, E. L. Thomas, M. G. Bawendi and M. F. Rubner, "Electroluminescence from heterostructures of poly (phenylene vinylene) and inorganic CdSe nanocrystals", *J. Appl. Phys., 83, 7965 (1998).*
16. A. Uddin, C. B. Lee, X. Hu, T. K. S. Wong and X. W. Sun, "Effect of doping on optical and transport properties of charge carriers in Alq_3","Effect of doping on optical and transport properties of charge carriers in Alq_3", *J. Crystal Growth 288 115(2006).*